ELSEVIER

Antiviral Research 53 (2002) 113–126

Antiviral Research

www.elsevier.com/locate/antiviral

The antiviral agent 5-chloro-1,3-dihydroxyacridone interferes with assembly and maturation of herpes simplex virus

P. Akanitapichat [1], K.F. Bastow *

Division of Medicinal Chemistry and Natural Products, School of Pharmacy, University of North Carolina at Chapel Hill, CB # 7630, Chapel Hill, NC 27599, USA

Received 14 August 2001; accepted 6 September 2001

Abstract

Antiviral drug screening and exploratory mechanistic work identified 5-chloro-1,3-dihydroxyacridone as a lead inhibitor of herpes simplex virus (HSV) replication, one without a primary effect on either HSV DNA or late viral protein synthesis (Antivir. Res. 45 (2000) 123). In this report, drug effects on viral DNA cleavage and packaging, HSV capsid production and virion morphogenesis in infected Vero cells were studied systematically in order to better localize the sensitive stage of the replication cycle. Maturation of replicating HSV DNA and virion production at late times were inhibited in the same dose-dependent fashion, suggesting that the drug might directly inhibit the cleavage and packaging processes. Based on density centrifugation analysis however, this possibility appears unlikely because overproduction of neither A- or B-capsids occurred upon drug treatment. Interestingly, similar studies coupled with either Western immunoblot or ultrastructural analysis showed that B-capsids with apparent normal protein composition accumulated at reduced levels (maximally about two- to three-fold) in drug-treated cells. Limited attempts to isolate drug-resistant viral mutants using standard approaches proved unsuccessful. In summery, 5-chloro-1,3-dihydroxyacridone inhibits one or more steps of HSV assembly since treatment results in reduced levels of capsids (particularly B-type) and reduced levels of encapsidated DNA. The action of the acridone derivative is an unusual one, with distinctive features when compared to a recently reported class of HSV encapsidation inhibitor and to the late replication defects of relevant viral mutants. © 2002 Published by Elsevier Science B.V.

Keywords: Acridone; Antiviral; Viral assembly

1. Introduction

Herpes simplex virus (HSV), can cause a variety of diseases in humans ranging in severity from mild, to debilitating, to life threatening. There are several efficacious drugs currently approved for treating HSV infection, with acyclovir and the prodrug valaciclovir being the most widely used. However, a significant risk of drug resistance

* Corresponding author. Tel.: +1-919-966-7633; fax: +1-919-966-0204.

E-mail address: ken_bastow@unc.edu (K.F. Bastow).

[1] Present address: School of Pharmacy, University of Ubonratchathanee, Warinchumrap Ampur, Ubonratchathanee 34190, Thailand.

0166-3542/02/$ - see front matter © 2002 Published by Elsevier Science B.V.
PII: S0166-3542(01)00203-0

occurs during therapy, especially for individuals with chronic viral infection and for the immunocompromized patient. To circumvent the problems associated with drug-resistant development, agents that act on novel biochemical targets continuously need to be discovered and developed (Bastow and Akanitapichat, 1997).

7-Chloro-1,3-dihydroxyacridone, a novel catalytic inhibitor of cellular DNA topoisomerase II (p170 isoform), is active against HSV replication (Bastow et al., 1994; Vance and Bastow, 1999). Evaluation of 1,3-dihydroxyacridone derivatives as enzyme inhibitors and as selective *anti*-HSV agents demonstrated that moving the chloro-substituent from the 7- to the 5-position (5-chloro-1,3-dihydroxyacridone; the structure is shown in Fig. 1) causes a loss of DNA topoisomerase II inhibitory activity but affords an increase in the compounds' selective antiviral activity. The 5-chloro congener is about 26-fold selective against HSV replication in Vero cells under a stringent assay condition (Akanitapichat et al., 2000). The same work also showed that the two isomeric compounds did not affect the accumulation of either viral DNA or late viral protein at effective antiviral concentrations and that continuous treatment initiated no later than 6 h after infection was required for maximum activity. Therefore, it was concluded that 1,3-dihydroxyacridone derivatives share an unusual and possibly a novel mechanism of action.

This report describes a detailed and systematic investigation of the antiviral blockade induced by the lead compound in HSV-infected Vero cells. It was found that inhibition of viral DNA cleavage and packaging by 5-chloro-1,3-dihydroxyacridone correlated with the inhibition of viral replication. This biochemical effect was judged to be a secondary response however, because drug treatment also reduced the amount of B-capsids (mutants defective in cleavage/packaging cause increased production of either A- or B-capsids as discussed in Section 4). Interestingly, the protein composition of B-capsids appeared normal and using two complementary approaches, the levels of B-capsids in drug-treated cells were estimated only to be two- to three-fold lower. Based on the present findings and current understanding of the capsid assembly and maturation pathways, plausible biochemical mechanisms that could account for the antiviral activity of the acridone derivative are considered.

2. Material and experimental procedures

2.1. Reagents and drugs

5-Chloro-1,3-dihydroxyacridone was synthesized as described (Akanitapichat et al., 2000) and prepared for biological evaluation as a 20 mM stock in dimethylsulfoxide. The polyvalent, polyclonal rabbit *anti*-HSV serum (76/7 VIII) was a generous gift of Professor T.A. Minson (Cambridge University). All other chemicals and reagents were obtained from commercial sources as indicated.

2.2. Cells and virus

The African green monkey kidney cell line (Vero 76, ATCC number CRL 1587) was obtained from the tissue culture facility of the UNC Lineberger Comprehensive Cancer Center (Chapel Hill, NC). Cells were propogated in RPMI-1640 supplemented with 5% (v/v) calf serum and 100 μg/ml of kanamycin (standard medium), in a humidified 5% CO_2 incubator at 37 °C. The HSV type 1 strain (KOS) was originally a gift of Professor Y.-C. Cheng (Yale University) and was not plaque-purified any time since receipt in 1990. A single working stock of the virus used for the studies reported herein was prepared using a low multiplicty infection as previously described (Bastow et al., 1994).

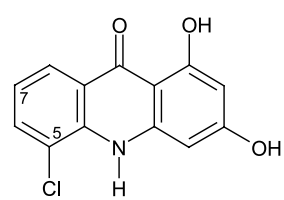

Fig. 1. Structure of 5-chloro-1,3-dihydroxyacridone.

2.3. Virus growth inhibition assay

The effect of drug treatment on viral growth was evaluated in matched cultures during all biochemical and analytical studies (Sections 2.4, 2.5 and 2.6), to permit a direct comparison between antiviral action and activity (the latter is dependent on several variables including viral load, cell growth status and serum concentration as reported previously Akanitapichat et al., 2000). For these viral growth measurements, confluent cell cultures were infected with the viral loads and using the treatment conditions specified in 'Results' (Section 3). In all experiments, the inoculate was removed at one hour post-infection and replaced with regular growth medium in the presence or absence of drug. Viral yield was measured by titration using a plaque assay (Bastow et al., 1994).

2.4. Evaluation of drug effects on viral DNA maturation

For each determination, confluent cultures (a T-25 cm^2 flask/sample, about 1×10^6 cells) were infected with virus at a multiplicity of 10 pfu per cell. Cell pellets were collected at 18 h post-infection by careful rinsing in ice-cold phosphate buffered saline (PBS), followed by scraping and low-speed centrifugation ($500 \times g$ for 5 min). Drained cell pellets were rapidly suspended in a 37° C solution of 1% (w/v) low-melting temperature agarose (FMC, Rockland, ME) in PBS and cast in duplicate plugs as described (Bastow et al., 1997). For DN'ase I treatment, one of the plugs was processed and treated with enzyme (Boehringer Mannheim, Indianapolis, IN) as previously described (McNab et al., 1998). Both the nuclease-treated and matched control plugs were then treated with proteinase K (1 mg/ml) at 50 °C for 48 h in 1% (w/v) laurylsarcosine, 0.4 M EDTA (pH 8). Processed plugs were washed two times for 15 min in 20 mM Tris–HCl (pH 7.5) and 50 mM EDTA (pH 8) at room temperature, placed against a gel comb then permanently mounted in place using a molten (50 °C) agarose gel solution (1% w/v) prepared in $0.5 \times$ TBE (25 mM Tris–HCl (pH 8.0), 25 mM boric acid and 0.5 mM EDTA). After gelling and the remainder of the gel was formed, DNA was separated by pulse field gel electrophoresis (PFGE) using a contor-clamp homogeneous electric field apparatus (CHEF) with an hexagonal electrode array. PFGE was in $0.5 \times$ TBE buffer at 120 V at 4 °C for 40–44 h, with a pulse time of 15 s. After separation, DNA was photo-nicked in situ with ultra violet light for 10 min, denatured by soaking the gel in 0.5 M NaOH and 1.5 M NaCl for 30 min, and neutralized in 1 M ammonium acetate and 0.002 M NaOH for 1 h. The DNA was transferred to a supported nitrocellulose membrane (Optitran®, Schleicher and Schuell, Keene, NH) in $10 \times$ SSC by vacuum blotting (TransVac™ Hoefer Scientific Instruments, San Francisco, CA) for 20 min. Denatured DNA was hybridized with a [^{32}P]-labeled *Bam* HI-digested genomic probe prepared from HSV (KOS) infected cells using rapid small-scale isolation (Kinter and Brandt, 1994), restriction and then random primed DNA labeling (using a commercial kit, Boehringer Mannheim, Indianapolis, IN). The hybridization and washing conditions used were as described (Bastow et al., 1986). Amounts of hybridized DNA were measured by quantitative phosphoroimaging using a STORM™ 860 Fluorimager and ImageQuant™ software according to the manufacturer's instruction (Molecular Dynamics, Sunnyvale, CA). A recent report states that the Kintner and Brandt method does not remove cellular DNA completely (Orlando et al., 2000) and the probe used in the present study was found to hybridize with cellular DNA sequences (Fig. 2A). Details of the approach used to normalize data are described in Section 3.1. Using these techniques, the packaging efficiency of cells (the proportion of cleaved viral DNA that was nuclease resistant) was estimated to be 6% at 18 h post-infection (range of 1–17%, six independent experiments). The reason for the low efficiency is unknown although sampling at a late stage of infection may be a factor. The factor (s) influencing encapsidation efficiency was not resolved although washing temperature (range 4–45 °C) and duration of nuclease treatment

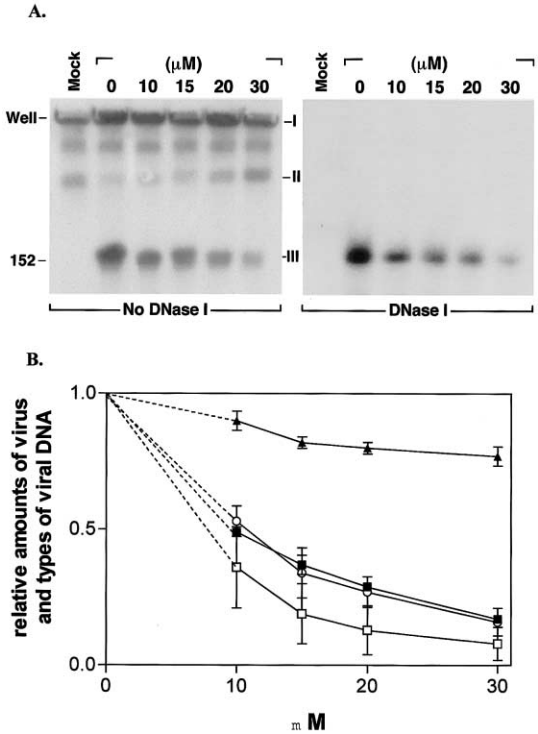

Fig. 2. Effect of 5-chloro-1,3-dihydroxyacridone on HSV DNA maturation. Vero cells were infected and processed for PFGE analysis as described (Section 2.4). Scanned images of autoradiographic results (A) obtained without DNA'se treatment (left panel) and with the nuclease processing step (right panel) are shown. Quantitative results of three independent experiments analyzed by phosphoroimaging and of antiviral activity measured concurrently in parallel cultures (B). Graphed results show drug effects on; viral yield (□); on replicative intermediates (band I, ▲); on cleaved and packaged DNA (band III, ■) and on (nuclease-resistant) packaged DNA (○). Inhibition of total viral DNA (measured as the sum of band I and III) by 30 μM drug was $40 \pm 10\%$ (2) which was not statistically different ($P > 0.05$; two-tailed unpaired t-test) from the reported value of $20 \pm 5\%$ (3) measured using conventional methods (Akanitapichat et al., 2000). Multiple comparisons of quantitative data (2B) using one-way ANOVA with Tukey's post-test showed the responses of viral yield, cleaved and packaged DNA (form III) and encapsidated DNA to drug-treatment were not significantly different ($P > 0.05$) from each other.

(15–100 min) were not confounding experimental variables (data not shown). Despite variable packaging efficiencies between experiments, the relative effects of drug treatment were reproducible (Fig. 2B).

2.5. Evaluation of drug effects on capsid and viral particle formation

To examine capsid production using rate-zonal sedimentation, capsids were isolated from infected cells and analyzed according to a published procedure with only minor modification (Sherman and Bachenheimer, 1988). For each determination, cultures (two T-225 cm^2 flasks/sample, about 4×10^7 cells) were infected at a multiplicity of 10 pfu per cell and incubated at 37° C for 20 h. One duplicate culture was treated continuously with the drug beginning at 1 h post-infection. Infected cultures were then scraped and the cell pellets were suspended in ice-cold buffer (80 mM KH_2PO_4, 300 mM NaCl and 1% (v/v) Nonidet P-40). After 3 min on ice, cells were ruptured by three cycles of freeze-thawing. The matched cell extracts were clarified by low-speed centrifugation ($1000 \times g$ for 5 min), then each supernatant was layered onto an 11.5 ml 15–50% (w/v) sucrose gradient and centrifuged for 1 h at 24 000 rpm at 4 °C using a Beckman SW 41 rotor. Capsid bands were visualized by light-scattering and photographed (representative qualitative results are shown in Fig. 3). The major capsid band (B-type) was collected in a volume of 3 ml by side puncture using a sterile syringe equipped with a 23-guage, 1.5 inch needle and the protein composition of matched capsid preparations was subsequently analyzed for semi-quantitative and qualitative drug effects on capsid production (Section 2.6). The A- and C-capsids were also collected and their protein composition analyzed using silver staining on a single occasion in order to verify assignment of the scaffolding protein VP22a (Section 2.6).

Ultrastructural analysis was used on a single occasion in order to confirm quantitative drug-effects on capsid production. Additional data from the same experiment allowed the sub- and extracellular distributions of viral particles to be visualized and qualitatively assessed. Confluent cell cultures were infected at a multiplicity of 10 pfu per cell for 18 h. Following a rapid rinse with serum-free medium, confluent cell cultures were fixed in situ with 3% glutaraldehyde for several hours followed by post-fixation in potassium fer-

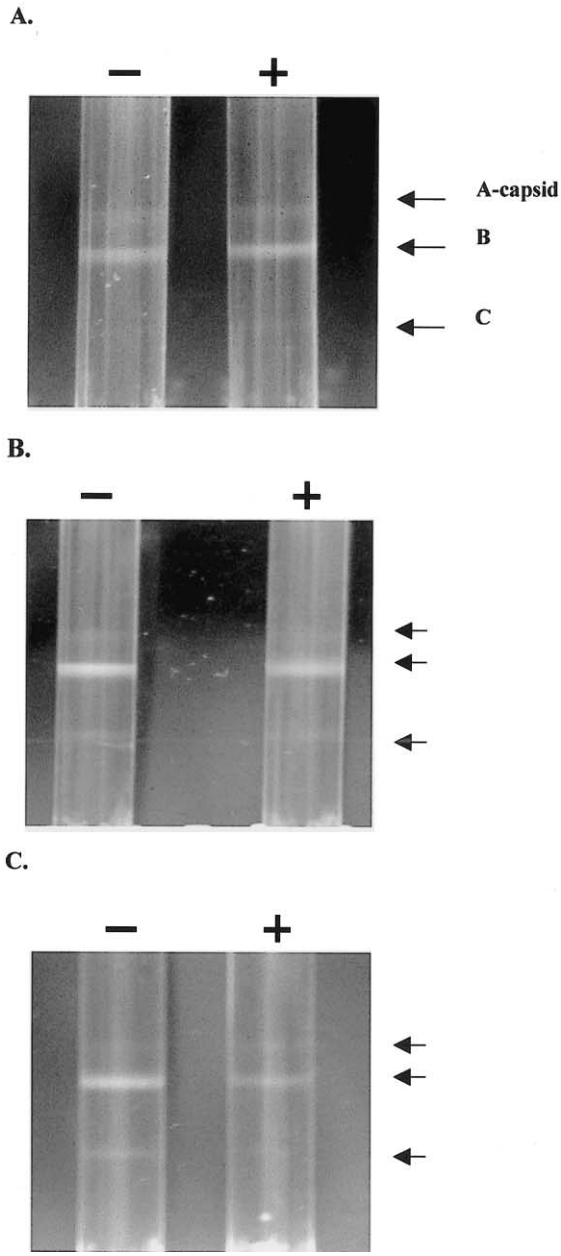

Fig. 3. Effects of 5-chloro-1,3-dihydroxyacridone on capsid formation. Vero cells were infected and processed for rate zonal centrifugation as described (Section 2.5) Representative density gradients of drug treated (+) and matched control (minus) are shown for 10, 15 and 30 μM in panels A–C, respectively. The inhibition of viral replication was measured concurrently (see Table 2). Capsid bands were identified as being either A-, B- or C-type according to the standard designation (Gibson and Roizman, 1972).

rocyanide-reduced osmium for 1 h (Russell and Burguet, 1987). After dehydration in a graded series of ethanols, preparations were infiltrated and embedded in Polybed-812 resin (Polyscience Inc., Warrington, PA). Ultrathin (70 nm) sections were cut *en face* to the substrate. Grid-mounted sections (four grids per treatment sample with several sections per grid) were double stained using uranyl acetate and lead citrate and the stained sections (each containing 30–50 cells) were analyzed using a Zeiss 910 transmission electron microscope operating at an accelerating voltage of 80 kV (LEO Electro Microscopy Inc., Thornwood, NY). For qualitative analysis, 25 × 30 cm photomicrographs (2000 and 2500 times magnification) of fields selected randomly were examined for numbers of nuclear-capsids and for enveloped viral particles in sub- and extra-cellular locations using a 3 × magnifying glass. Cytoplasmic capsids could not be reliably scored using the same images because electron dense material and cytoplasmic inclusions confounded precise analysis. However, inspection of images obtained at higher magnification (20 000–31 500 times) showed that A- and C-capsids were the predominant type located in the cytoplasm of infected cells and their number was substantially reduced but not eliminated upon drug-treatment (data not shown). Representative photomicrographs and composites are shown in Fig. 4. For quantitative analysis, at least 40 nuclei randomly selected from each sample were captured as digital images using a Gatan MSC camera with DigitalMicrograph. High resolution (1024 × 1024 pixel) images taken at 8000 and 16 000 times magnification were manually scored for capsid arrays and capsids and the latter data was subjected to statistical analysis. Although the ultrastructural study was limited to a single experiment, the quantitative results obtained (Table 1) were entirely consistent with the findings of complementary biochemical and virological studies (Section 3).

2.6. Preparation and analysis of B-capsid proteins

Matched samples of B-capsids collected from sucrose gradients (Section 2.5) were denatured by the addition of standard SDS-PAGE sample

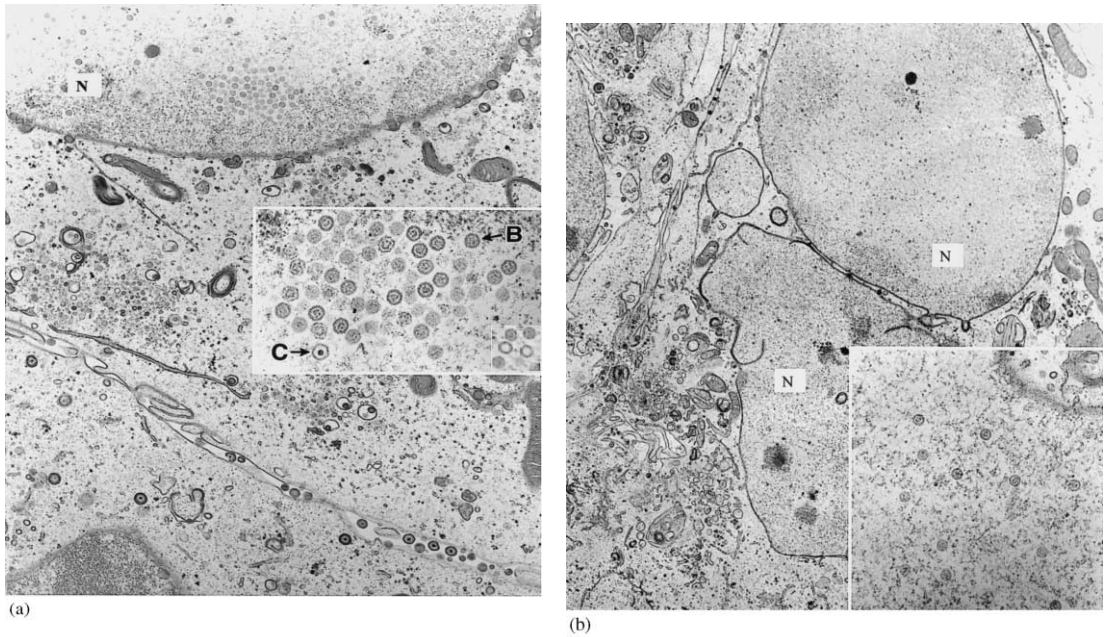

Fig. 4. Effects of 5-chloro-1,3-dihydroxyacridone on capsid and viral particle formation. Thin sections of infected cells were viewed using transmission electron microscopy (Section 2.5) and representative sample fields either in the absence (A) or presence of drug (B; 30 μM) are shown. Viral yield measured concurrently showed that replication was inhibited to 7% of control by drug-treatment. Labeled arrows in the large inset show representative B- and C-capsids. The small inset shows three B-capsids and two A-capsids. The capsid arrays detected in about one-third of control nuclei and visible in Fig. 4A is duplicated in the inset of the same as a five-fold magnified image. Enveloped viral particles are clearly visible in the extracellular space. The inset of Fig. 4B shows dispersed nuclear capsids, the only type of capsid distribution observed in drug-treated samples. A limited quantitative analysis of the ultrastructural data is given in Table 1.

buffer and heating at 95 °C for 5 min. Proteins were resolved on a 16 cm 10% polyacrylamide-SDS separating gel using a Protean® IIxi cell (Biorad, Richmond, CA) and the standard method (Laemmli, 1970). Protein concentration was too low to be determined accurately so, to avoid potential problems associated with sample concentration and recovery, protein composition was compared directly by loading equal volumes of matched samples. Consequently, the analysis using immune detection was only semi-quantitative because comparison assumes a similar recovery of gradient-purified capsids. For immune detection of viral capsid proteins, electrophoresed samples were transferred to PVDF membranes (NEN products, Boston, MA) using a Trans Blot semi-dry cell (Bio-Rad, Hercules, CA) according to the manufacturer's instructions. The membrane was first blocked in TBST buffer [10 mM Tris–HCl (pH 7.5), 150 mM NaCl and 0.05% Tween 20] containing 20% (w/v) dried milk (Carnation®). After blocking, the blot was treated sequentially with a primary antibody against infected cell proteins (1/10 000 dilution) and with *anti*-rabbit IgG (Fc) alkaline phosphatase conjugate according to the manufacturers recommendation (Promega, Madison, WI). The basis for assigning core and shell capsid proteins is given in the legend of Fig. 5 however, mono-specific antibodies were not used for immune detection so the assignments are firm but not absolute. Interestingly, other proteins in the vicinities of VP21 and VP22a were detected (Fig. 5) but the significance of this observation is not known. Relative

amounts of three capsid proteins (VP21, VP22a and VP23) were measured using an enhanced fluorescence detection system according to the manufacturer's instruction (Amersham, Cleaveland, Ohio) and fluorimaging analysis was performed as described in Section 2.3. Results of the analysis are given in Table 2. The direct visualization of total proteins present in capsid preparations (Fig. 5A) was achieved by ultra-sensitive silver-staining of gels (Merril et al., 1983)

2.7. Approaches to isolate drug-resistant virus

A limited series of experiments using two approaches were used to enrich for pre-existing variants. First, virus was passaged four times at low multiplicity (0.01 pfu per cell) in the presence of 5 μM 5-chloro-1,3-dihydroxyacridone. Cultures with extensive cytopathic effect were harvested and virus produced was measured prior to the next passage step. The recent use of a serial low-passage method proved successful for generating resistance to HSV encapsidation inhibitors (Van Zeijl et al., 2000; Section 4) and to acyclovir (Chen et al., 1998). Direct selection for growth in 30 μM of the acridone derivative was also explored by infecting multi-well cultures with 0.02 pfu per cell. After 3 days, one culture showing significant cytopathic effect was harvested and virus was measured. The population was passaged twice then plaque-purified once under selection (15 μM) to generate two isolates for evaluation (Section 3.5).

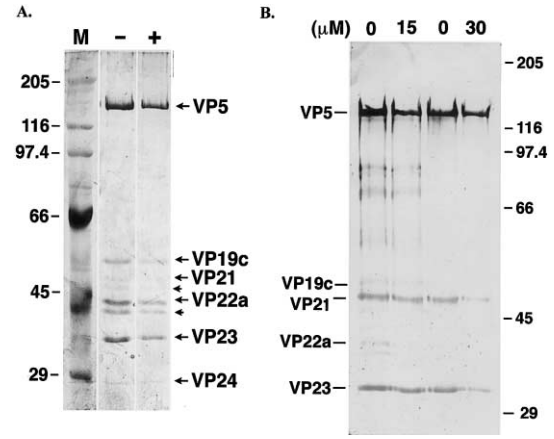

Fig. 5. Effect of 5-chloro-1,3-dihydroxyacridone on the protein composition and amount of B-capsids. Preparations from matched pairs of gradients were analyzed as described in Section 2.6. Proteins were visualized directly by silver-staining (A). Viral proteins are indicated in the right margin. Three capsid shell proteins (VP5, VP19c, VP23) and a core protein (VP24) were assigned based on molecular mass and reactivity with an HSV-specific polyclonal antibody (Panel B; Rixon, 1993; Desai et al., 1994). The assignment of VP22a was also based on the inability to detect this internal scaffolding protein in A- and C-capsids preparations using an ultra-sensitive silver-stain (data not shown). The viral protease (VP24) and the minor capsid protein (VP26; 12 kDa) were detected in all samples and were assigned based on apparent molecular weight, however VP26 is not shown in the cropped image (Fig. 5A). The two short arrows label the proteins of unknown origin (Section 2.6). The lane denoted by '+' is the matched preparation of cells treated with 10 μM drug. Molecular weight markers in kDa are shown in the left margin. Non-adjacent lanes from a single gel were juxtaposed to create the image in panel A. In panel B, a representative immunoblot of B-capsid proteins is shown. The relative amounts of VP21, VP22a and VP23 in this and another experiment were measured using fluorimaging and semi-quantitative results of the analysis are given in Table 2.

Table 1
Quantitative ultrastructural analysis of HSV capsids in Vero cell nuclei

Parameter	Drug concentration (mM)		
	0	15	30
No. of nuclei counted	43	40	41
No. of nuclei with visible capsids	43	38	40
No. of capsids/nucleus[a]	97 ± 14	57 ± 12[b]	36 ± 4[b]
Number of nuclei with capsid arrays[c]	12	0	0
Viral replication (% control)	100	20	7

[a] Values are mean ± SEM.

[b] The amount of nuclear capsids in drug-treated cells were compared to the control and to each other using a two-tailed unpaired *t*-test, The reduction in mean capsid number was significant at 15 μM ($P = 0.0366$) and highly significant for the 30 μM treatment ($P = 0.0001$). However, the mean values for drug-treatment were not significantly different from each other ($P = 0.078$).

[c] The sections of nuclei scored positive contained arrays ranging in number from one to seven with three capsid arrays being the average number per nucleus.

2.8. Statistical analysis

The program Prism™ version 3 (Graphpad Software, Inc., Sand Diego, CA) was used for graphing and statistical analysis of study results.

3. Results

3.1. Effect of 5-chloro-1,3-dihydroxyacridone on viral DNA maturation

Replicating HSV DNA is concatameric and starting between 4 and 6 h post-infection, replication intermediates are cleaved at sites defined by specific *cis*-acting signals in order to generate the 152 kb genomic DNA for encapsidation (Roizman, 1996). Separation of the mature unit-length DNA from replicative intermediates can be achieved using PFGE, as demonstrated in several studies (Zhang et al., 1994; Martinez et al., 1996; McNab et al., 1998). The encapsidated viral DNA is nuclease-resistant, unlike either cellular DNA, or replicating viral DNA or abortively cleaved viral DNA (Lentine and Bachenheimer, 1990). Therefore, treatment of cells with and without DN'ase I prior to removal of protein and PFGE separation was the approach used to examine whether the acridone derivative affected the levels of abortively cleaved and, or encapsidated DNA's in cells at a late time of infection. As shown in the left panel of Fig. 2A, several hybrids were detected in the infected control sample prepared without DN'ase treatment. The upper species (band I) did not enter the gel and it is a mixture of replicating viral DNA and cellular DNA, since a signal was always detected in mock-infected plugs (presumably due to probe contamination discussed in Section 2.4; compare mock and no drug treatment lanes of Fig. 2A). Thus, the amount of replicating viral DNA was estimated by subtracting the signal in the matched mock-infected sample from the signals of each virus-infected sample. The two species of intermediate mobility are presumably cellular DNA also, since they were detected in all six samples shown in the left panel of Fig. 2A, however, the upper band was not reproducibly resolved using PFGE (data not shown). Therefore, the relative intensity of band II (the lower one) was routinely used to normalize between samples for load variation and transfer efficiency. Analysis of hybridization data using the two manipulations described above appeared to be valid because drug effects on viral DNA accumulation measured using the PFGE approach were similar to those measured using a traditional DNA isolation method followed by conventional gel electrophoresis and Southern blotting (Fig. 2 legend). The highest mobility hybrid (band III) was detected exclusively in the infected samples (left panel of Fig. 2A) and it co-migrated with the DNA of virions purified from culture fluid (data not shown). Therefore, band III represents the 152 kb progeny viral DNA that was either abortively processed from replication intermediates or successfully processed and encapsidated at time of harvest. In the DN'ase-treated infected control, only a single species that co-migrated with band III was detected and because it was nuclease resistant, it represents the fraction of cleaved DNA that was processed and packaged successfully (right panel of Fig. 2A). Interestingly, the mobility of mature viral DNA (band III) was similar in all infected samples suggesting that, within the limited resolution of the analytical approach, neither the length or structure of progeny DNA was affected by drug treatment. Statistical analysis of quantitative data from replicate experiments showed that dose-dependent decreases of cleaved viral DNA and of

Table 2
Effects of 5-chloro,1,3-dihydroxyacridone on B-capsid proteins and viral replication

Parameter	Drug concentration (μM)		
	10	15	30
Amount of B-capsid proteins (% control)[a]	84 ± 1	60 ± 1	30 ± 5
Viral replication (% control)	50	19	4

[a] Amounts of VP21, VP22a and VP23 in B-capsid preparations were compared between drug-treated and a matched infected control using enhanced fluorescence imaging of Western immunoblots (Section 2.6 and Fig. 5B). Values are the mean and standard deviation for relative amounts of the three capsid proteins analyzed.

encapsidated DNA closely paralleled the inhibition of viral growth by the drug (Fig. 2B and legend). These correlations indicate that 5-chloro-1,3-dihydroxyacridone interferes with the maturation of replicated viral DNA but does not do so by inducing abortive cleavage of the replication intermediate. The overall result suggests the possibility that direct inhibition of viral encapsidation occurs in drug-treated cells

3.2. Drug effects on capsids detected using rate-zonal centrifugation

Three principal types of capsid can be readily isolated from productively infected cells and these are denoted as A-, B- and C-capsids, respectively. The B-Capsid is composed of seven viral proteins designated as VP5, VP19c, VP21, VP22a, VP23, VP24 and VP26 (Rixon, 1993; Homa and Brown, 1997). The process of viral DNA packaging causes a selective loss of VP21 and VP22a and results in the formation of either A- or C-capsids. The former type is devoid of viral DNA and is generally considered to be the end product of abortive DNA packaging. Indeed, either A- or B-capsids accumulate in cells infected with cleavage and packaging viral mutants. Unlike A- and B-capsids, the C-capsid contains a progeny viral DNA molecule and is therefore a product of a successful cleavage and packaging event. Therefore, B-capsids are thought to be precursors of both A- and C-capsids. Since 5-chloro-1,3-dihydroxyacridone interfered with viral DNA maturation (Fig. 2), specific effects on viral capsid production were anticipated (for additional discussion of this and related points, see Section 4). The three capsid types can be readily distinguished based on particle density, typically studied using rate-zonal ultracentrifugation and on capsid morphology in electronmicrographs. These two analytical methods are complementary and both of them were used in the present work to evaluate drug effects on viral particle formation. Density centrifugation was used as an initial approach and photographs of representative gradients and a depiction of the overall findings are given in Fig. 3. As shown, rate-velocity sedimentation of matched infected control preparations typically yielded three bands corresponding to the three capsid varieties (Fig. 3A–C). The B-capsids always were the predominant species while A- and C-capsids were relatively minor constituents and C-capsids in particular were only faintly visible in some of the experiments. Treatment with drug at 10 μM had marginal qualitative effects on capsid production, even though viral replication was inhibited by 50% (Fig. 3A and Section 3.4). Although the initial approach used to investigate capsid production has a low sensitivity, a clear and reproducible decrease in the relative amount of B-capsids was observed for the 15 μM treatment and levels of B-capsids and to a lesser extent C-capsids were reduced when the drug concentration was further increased to two-fold (Fig. 3B and C, respectively). Interestingly, amounts of A-capsids appeared to be unaffected by any drug-treatment (Fig. 3A–C). A semi-quantitative analysis of B-capsid proteins supported the conclusion that 5-chloro-1,3-dihydroxyacridone reduced the amounts of B-capsids and showed that they were lowered at all concentrations of the drug tested (Section 3.4). Although the apparent reduction of C-capsids at the highest drug concentration (Fig. 3C) is compatible with the observed perturbation of viral encapsidation (Fig. 2B), the reduction of B-capsids was unexpected and as will be discussed (Section 4), it suggests that 5-chloro-1,3-dihydroxyacridone does not act as a specific encapsidation inhibitor.

3.3. Ultrastructural analysis of drug effects on viral assembly

To directly investigate drug effects on viral assembly, infected cells were analyzed using transmission electron microscopy and findings were compared to results of PFGE and rate-zonal centrifugation experiments. Representative electron micrographes are shown in Fig. 4 and results from a quantitative analysis of nuclear capsids are given in Table 1. Thin sections of control infected cells prepared at a late time of infection contain all three capsid types as well as enveloped parti-

cles (Fig. 4A). The C-capsids were predominantly located in the cytoplasm of the infected cell (Section 2.5). In infected cell nuclei, capsids with electron translucent cores (B-type) were either distributed throughout or they formed array-like structures (insert of Fig. 4A, Table 1). Similar capsid formations in Vero cells were designated as 'assemblons' and include proteins of both immature and mature capsids as well as some tegument proteins (Ward et al., 1996). The viral assemblon was postulated to be a functional intracellular site of the cleavage and packaging process [although this interpretation was recently disputed (Lamberti and Weller, 1998)]. For infected cells treated with either 15 μM (data not shown) or 30 μM of the acridone derivative (Fig. 4B), a significant two- to three-fold reduction of nuclear capsids (predominantly B-type) was measured (Table 1). Numbers of C-capsids were not scored (Section 2.5) however, inspection of highly magnified images showed drug-treatment substantially reduced relative amounts without completely eliminating them (data not shown). Therefore, drug effects detected using transmission electron microscopy were in good agreement with results obtained using PFGE and velocity sedimentation analyses (Fig. 2B and Fig. 3, respectively). The ultrastructural analysis also showed that numbers of enveloped particles were reduced in infected cultures treated with 15 and 30 μM of the drug, particularly those normally located in the extracellular compartment (data not shown). These qualitative observations are consistent with the effect of 5-chloro-1,3-dihydroxyacridone on productive infection and with viral replication being blocked at a late stage but prior to envelopment. Interestingly, the nuclear capsid arrays detected in about one-third of controls (inset of Fig. 4A and Table 1) were not observed in drug-treated samples. Rather, the majority of B-capsids were always found distributed diffusively throughout nuclei of drug-treated cells (inset of Fig. 4B) much like the situation seen in the majority of infected control nuclei (Table 1). The overall result obtained using transmission electron microscopy support the interpretation that 5-chloro-1,3-dihydroxyacridone interferes with some stage(s) of capsid maturation.

3.4. Protein composition of B-capsids isolated from drug-treated cells

The abnormal encapsidation in drug-treated cells (Section 3.1) could be a secondary effect due to alterations in location and, or structure and, or protein composition of B-capsids, rendering them non-competent for viral DNA packaging (for a rationale and additional discussion see Section 4). The third possibility was investigated. Capsid proteins were analyzed qualitatively, using SDS-PAGE and silver staining and also semi-quantitatively, using antibody detection on Western blots. As shown in Fig. 5A, B-capsids isolated from infected cells treated with compound (10 μM) contained similar viral proteins as B-capsids prepared from control infected cells, but the former were less abundant based on their relative staining intensity (presumably reflecting the reduced amounts of capsids in the sample). Importantly, the core proteins VP21, VP22a and VP24 were detected in B-capsids isolated from drug-treated cells showing that the proteolytic processing steps of the capsid maturation pathway were not affected. A semi-quantitative analysis of B-capsid preparations using Western immunoblot (Fig. 5B) revealed the following: capsid shell and internal proteins were coordinately reduced in preparations from drug-treated cells, the effect was a dose-dependent one and the magnitude of the effects were similar to those measured in the single ultrastructural study (Table 1). The overall findings confirm that B-capsids were significantly under-produced upon drug-treatment and also demonstrate that critical proteolytic processing steps of capsid maturation were not blocked by the acridone derivative.

3.5. Selection of drug-resistant virus

A limited series of experiments to isolate viral variants resistant to 5-chloro-1,3-dihydroxyacridone were conducted using standard approaches (Section 2.7). Enrichment from the viral population growing under drug-selection (5 μM) proved unsuccessful but a small plaque variant and a syncitial (*syn*-) isolate were ultimately obtained from a sub-population generated by direct selec-

tion at a six-fold higher concentration. However, neither isolate exhibited reproducible levels of resistance upon repeated testing for either drug susceptibility (plaque elimination assay) or for biochemical changes (PFGE analysis). In contrast, variants that produced normal-sized plaques in the presence of 7.5 μM acyclovir (15 times the ED_{50}, value) were isolated directly from the population (data not shown). The overall result shows that HSV cannot readily develop stable resistance to 5-chloro-1,3-dihydroxyacridone.

4. Discussion

This report demonstrates an important biochemical effect of treating HSV-infected cells with 5-chloro-1,3-dihydroxyacridone is the interference with viral DNA maturation since a dose-dependent decrease in encapsidated DNA closely paralleled the inhibition of viral replication (Fig. 2B). Moreover, the qualitative reductions of C-capsids detected in density gradient and ultrastructural experiments were consistent with a drug-induced perturbation of cleavage and packaging. Numerous studies involving HSV-1 mutants have helped define the viral cleavage and packaging machinery and have illustrated the complexity of the process although it is not yet well understood at the biochemical level. However, it is established that seven viral proteins, products of the *UL6*, *UL15*, *UL17*, *UL25*, *UL28*, *UL32* and *UL33* genes, as well as competent B-capsids are all required for successful cleavage and packaging of viral DNA (Preston et al., 1983; Addison et al., 1984, 1990; Sherman and Bachenheimer, 1987; Weller et al., 1987; Al-Kobaisai et al., 1991; Desai et al., 1993, 1994; Gao et al., 1994; Baines et al., 1997; Lamberti and Weller, 1998; McNab et al., 1998; Salmon et al., 1998). Defects in five of the essential viral functions (other than the *UL25* gene product) or the formation of B-capsids that are not competent can result in a failure of the normal cleavage and packaging process. Cells infected with cleavage and packaging mutants synthesize viral DNA normally but replicating DNA cannot mature so C-capsids are not produced and B-capsids accumulate. In UL25 mutant-infected cells, replicating viral DNA can be cleaved normally but cannot be packaged successfully, giving rise to an increase in A-capsids and an absence of C-capsids (McNab et al., 1998). By comparison to the phenotypes of cleavage/packaging mutants outlined above, 5-chloro-1,3-dihydroxyacridone has unusual effects on capsid production because the drug reduces the amount of both B- and C-capsids and the agent does not affect levels of A-capsids (Fig. 3B and C; Table 1). Novel thiourea compounds were recently described as lead inhibitors of HSV-1 cleavage and encapsidation (Van Zeijl et al., 2000). Studies using drug-resistant mutants showed that the agents target the *UL6* gene product and that they completely prevented encapsidation and C-capsid production based on PFGE and ultrastructural analyses, respectively (effects on A- and B-capsids were not reported). Therefore, the action of the 5-chloro-1,3-dihydroxyacridone is distinctive because complete inhibition of encapsidation was not observed and C-capsids were detected but were under-produced. Another difference between the action of acridone and thiourea derivatives is that capsid arrays were detected in nuclei of Vero cells treated with the latter. The comparisons outlined above and the significant differences noted suggest that 5-chloro-1,3-dihydroxyacridone does not directly interfere with the function(s) of any one of the cleavage and packaging proteins.

As noted (Section 2.3), B-capsids are composed of seven viral proteins including VP5, VP19c, VP21, VP22a, VP23, VP24 and VP26. The core proteins, VP21/VP24 andVP22a are encoded by the *UL26.5* and *UL26* genes, respectively (Rixon, 1993; Homa and Brown, 1997). For encapsidation to occur, the precursors of VP22a and VP21 are cleaved by the protease precursor (the *UL26* gene product), resulting in small-cored B-capsids. Although large- and small-cored B-capsids are both typically produced in the infected cell, the latter type is the major species. In protease mutant-infected cells, preVP22a and, or protease precursor are unable to be processed, giving rise to accumulation of large-cored B-capsids and capsid aggregation (Preston et al., 1983; Gao et al., 1994; Trus et al., 1996; Register and Shafer, 1997). Moreover, aberrant capsid structures were observed in cells

infected with a UL26/UL26.5 mutant (Desai et al., 1993). By way of comparison to known phenotypes of capsid maturation mutants, the cleavage products VP21, VP22a and VP24 were detected in B-capsids prepared from drug-treated cells (Fig. 5) and neither capsid aggregation or aberrant capsid structures were detected (Fig. 4b). Large- and small-cored B-capsids were not enumerated because it is difficult to distinguish between them with precision based on morphology alone. However, present findings suggest that small-cored B-capsids assemble in drug-treated cells but they are not competent for encapsidation and they accumulate at reduced levels.

The partial reduction in levels of B-capsids at effective antiviral concentrations is an unusual and previously unreported feature of antiviral drug treatment. Based on current models of HSV capsid assembly and maturation, two plausible mechanisms to account for the antiviral activity of 5-chloro-1,3-dihydroxyacridone are considered. The reduction of B-capsids (and consequently C-capsids) upon drug treatment is qualitatively (but not quantitatively) similar to the phenotype of capsid assembly (VP5, VP19c and VP23) mutants (Weller et al., 1987; Person and Desai, 1998). Abnormal capsid production by assembly mutants occurs because an essential capsid shell protein is not produced but it was shown previously that the synthesis and steady-state accumulation of viral late proteins is apparently unaffected by the acridone derivative (Akanitapichat et al., 2000). Although amounts of capsid proteins were probably not limiting for efficient capsid assembly, this possibility awaits more rigorous testing. For example, neither VP5 nor VP23 can localize into the nucleus independently (Homa and Brown, 1997). Interaction of VP5 with preVP22a as well as interaction of VP23 and VP19c in the cytoplasm is critical for the nuclear import of VP5 and VP23. Therefore, it is conceivable that 5-chloro-1,3-dihydroxyacridone could perturb the nuclear import of capsid proteins and this might explain inefficient capsid assembly (although it is unclear why a two- to three-fold reduction in B-capsids essentially results in a complete inhibition of productive infection). A second possible mechanism is that capsid maturation is blocked at a late step, rendering B-capsids non-competent to package viral DNA. For example, an elegant study using a temperature-sensitive protease mutant (*ts* prot.A) recently demonstrated the existence of two distinct structural forms of polyhedral capsids and an ATP-dependent transformation step (Dasgupta and Wilson, 1999). The two capsid varieties contain the cleavage products of the protease precursor (VP21, VP22a and VP24) but can be distinguished based on differences in conformation-dependent epitopes on VP5, the major capsid protein. Dasgupta and Wilson showed that experimental manipulations, which block the formation of ATP-dependent capsids prevented encapsidation also. Therefore, an alternative working model to account for present findings is that 5-chloro-1,3-dihydroxyacridone interferes with ATP-dependent conformational change(s) and non-competent B-capsids accumulate as a consequence (although the observed decrease in B-capsids is not readily explained).

In summary, the antiviral action of 5-chloro-1,3-dihydroxyacridone is evidently a novel one. An important biochemical effect of the compound is interference with viral DNA maturation and this likely occurs as a consequence of an abnormal production of competent B-capsids. The precise mechanism of action was not defined in the present work and it may not be straightforward to elucidate. Assuming that the critical target is a single viral protein then identification using mutant characterization could be problematic because limited attempts to isolate variants resistant to 5-chloro-1,3-dihydroxyacridone were not successful. Since the compounds' action is distinct from either previously reported *anti*-HSV drugs or replication defects of relevant viral mutants, 5-chloro-1,3-dihydroxyacridone and its derivatives should be useful as tools for dissecting the complex steps of HSV assembly and maturation. However, further optimization of the acridone lead and identification of the primary biochemical target(s) will be essential for the development of a viable antiviral drug candidate.

Acknowledgements

This work was supported, in part, by a grant from the Pharmacy Foundation of NC, Inc., a University Faculty Research Grant (5-43393), and by a pre-doctoral scholarship from the Thai government (to P.A.). Special thanks to Professor J. Cannon and J.A. Dempsey (Microbiology department, UNC) for practical advice and use of the PFGE system and vacuum blotting apparatus. Dr Vicky Madden of the UNC Microscopy and Imaging core facility is also acknowledged for her expert guidance, training and help with TEM analysis. The work performed by P.A. was in partial fulfillment of the requirements for the degree of Doctor of Philosophy.

References

Addison, C., Rixon, F.J., Palfreyman, J.W., O'Hara, M., Preston, V.G., 1984. Characterization of a herpes simplex virus type 1 mutant which has a temperature sensitive defect in penetration of cells and assembly of capsids. Virology 138, 246–259.

Addison, C., Rixon, F.J., Preston, V.G., 1990. Herpes simplex type 1 UL28 gene product is important for the formation of mature capsids. J. Gen. Virol. 71, 2377–2384.

Akanitapichat, P., Lowden, C.T., Bastow, K.F., 2000. 1,3-Dihydroxyacridone derivatives as inhibitors of herpes virus replication. Antivir. Res. 45, 123–134.

Al-Kobaisai, M.F., Rixon, F.J., McDougall, L., Preston, V.G., 1991. The herpes simplex virus UL33 gene product is required for the assembly of full capsids. Virology 180, 380–388.

Baines, J.D., Cunningham, C., Nalwanga, D., Davison, A., 1997. The UL15 gene of herpes simplex type 1 contains within its second exon a novel open reading frame that is translated in frame with the UL15 gene product. J. Virol. 71, 2666–2673.

Bastow, K.F., Bouchard, J., Ren, X.J., Cheng, Y.C., 1986. Synthesis of dihydrofolate reductase and metabolism of related RNA in a methotrexate resistant human cell line infected with herpes simplex virus type 2. Virology 149, 199–207.

Bastow, K.F., Itoigawa, M., Furukawa, H., Kashiwada, Y., Bori, I.D., Ballas, L.M., Lee, K.H., 1994. Antiproliferative actions of 7-substituted 1,3-dihydroxyacridones; possible involvement of DNA topoisomerase II and protein kinase C as biochemical targets. Bio-org. Med. Chem. 2, 1403–1411.

Bastow, K.F., Wang, H.K., Cheng, Y.C., Lee, K.H., 1997. Synthesis and evaluation of camptothecin-4-β-amino-epipodophyllotoxin conjugates as inhibitors of mammalian DNA topoisomerases and of cell growth. Bio-org. Med. Chem. 5, 1481–1488.

Bastow, K.F., Akanitapichat, P., 1997. Antiviral agents, DNA. In: Wolf, M.E. (Ed.), Burger's Medicinal Chemistry and Drug Discovery. Wiley, New York, pp. 497–549.

Chen, H., Tang, L., Li, J.-N., Parke, R., Mold, D.E., Snabre, J., Hwu, J.R., Tseng, W., Hwang, R., 1998. Antiviral activity of methylated nordihydrogualaretic acids. 2. Targeting herpes simplex virus replication by the mutation-insensitive transcription inhibitor tetra-*O*-methyl NDGA. J. Med. Chem. 41, 3001–3007.

Dasgupta, A., Wilson, D.W., 1999. ATP depletion blocks herpes simplex virus DNA packaging and capsid maturation. J. Virol. 73, 2006–2015.

Desai, P., DeLuca, N.A., Glorioso, J.C., Person, S., 1993. Mutations in herpes simplex virus type 1 genes encoding VP5 and VP23 abrogate capsid formation and cleavage of replicated DNA. J. Virol. 67, 1357–1364.

Desai, P., Watkins, S.C., Person, S., 1994. The size and symmetry of B capsids of herpes simplex virus type I are determined by the gene products of the UL26 open reading frame. J. Virol. 68, 5365–5374.

Gao, M., Matusick-Kumar, L., Hurlburt, W., DiTusa, S.F., Newcomb, W.W., Brown, J.C., McCann, P.J. III, Deckman, L., Colonno, R.J., 1994. The protease of herpes simplex virus type 1 is essential for functional capsid formation and viral growth. J. Virol. 68, 3702–3712.

Gibson, W., Roizman, B., 1972. Proteins specified by herpes simplex virus: VIII. Characterization and composition of multiple capsid forms of subtypes 1 and 2. J. Virol. 10, 1044–1052.

Homa, F.L., Brown, J.C., 1997. Capsid assembly and DNA packaging in herpes simplex virus. Med. Virol. 7, 107–122.

Kinter, R.L., Brandt, C.R., 1994. Rapid small-scale isolation of herpes simplex virus DNA. J. Virol. Methods 48, 189–196.

Laemmli, U.K., 1970. Cleavage of structural proteins during the assembly of the head of bacteriophage T4. Nature 227, 680–685.

Lamberti, C., Weller, S.K., 1998. The herpes simplex type 1 cleavage/packaging protein, UL32, is involved in efficient localization of capsids to replication compartments. J. Virol. 72, 2463–2473.

Lentine, A.F., Bachenheimer, S.L., 1990. Intracellular organization of herpes simplex virus type 1 DNA assayed by staphylococcal nuclease sensitivity. Virus Res. 16, 275–292.

Martinez, R., Sarisky, R.T., Weber, P.C., Weller, S.K., 1996. Herpes simplex type 1 alkaline nuclease is required for efficient processing of viral DNA replication intermediates. J. Virol. 70, 2075–2085.

McNab, A.R., Desai, P., Person, S., Roof, L.L., Thomsen, D.R., Newcomb, W.W., Brown, J.C., Homa, F.L., 1998. The product of the herpes simplex type 1 UL25 gene is required for encapsidation but not for cleavage of replicated viral DNA. J. Virol. 72, 1060–1070.

Merril, C.R., Goldman, D., Van Keuren, M.L., 1983. Silver staining methods for polyacrylamide gel electrophoresis. Methods Enzymol. 96, 230–239.

Orlando, S.J., Nabavi, M., Gharakhanian, E., 2000. Rapid small-scale isolation of SV40 virions and SV40 DNA. J. Virol. Methods 90, 109–114.

Person, S., Desai, P., 1998. Capsids are formed in a mutant virus blocked at the maturation site of the UL26 and UL26.5 open reading frames of herpes simplex type I but are not formed in a null mutant of UL38 (VP19c). Virology 242, 193–203.

Preston, V.G., Coates, J.A.V., Rixon, F.J., 1983. Identification and characterization of a herpes simplex virus gene product required for encapsidation of viral DNA. J. Virol. 45, 1056–1064.

Register, R.B., Shafer, J.A., 1997. Alterations in catalytic activity and virus maturation produced by mutation of the conserved histidine residues of herpes simplex virus type 1 protease. J. Virol. 71, 8572–8581.

Rixon, F.J., 1993. Structure and assembly of herpesviruses. Semin. Virol. 4, 135–144.

Roizman, B., 1996. Herpes simplex viruses and their replication. In: Fields, B.N., Knipe, D.M., Howley, P.M. (Eds.), Fields Virology. Lippincott-Raven, Philadelphia, pp. 2231–2295.

Russell, L.D., Burguet, S., 1987. Ultrastructure of Leydig cells as revealed by secondary tissue treatment with a ferrocyanide: osmium mixture. Tissue Cell 9, 99–112.

Salmon, B., Cunningham, C., Davison, A.J., Harris, W.J., Baines, J.D., 1998. The herpes simplex type 1 UL17 gene encodes virion tegument proteins that are required for cleavage and packaging of viral DNA. J. Virol. 72, 3779–3788.

Sherman, G., Bachenheimer, S.L., 1987. DNA processing in temperature-sensitive morphogenic mutants of HSV 1. Virology 158, 427–430.

Sherman, G., Bachenheimer, S.L., 1988. Characterization of intranuclear capsids made by *ts* morphogenic mutants of HSV 1. Virology 163, 471–480.

Trus, B.L., Booy, F.P., Newcomb, W.W., Brown, J.C., Homa, F.L., Thomsen, D.R., Steven, A.C., 1996. The herpes simplex virus procapsid: structure, conformational changes upon maturation, and roles of the triplex proteins VP19c and VP23 in assembly. J. Mol. Biol. 263, 447–462.

Vance, J.R., Bastow, K.F., 1999. Inhibition of DNA topoisomerase II catalytic activity by the antiviral agents 7-chloro-1,3-dihydroxyacridone and 1,3,7-trihydroxyacridone. Biochem. Pharmacol. 58, 703–708.

Van Zeijl, M., Fairhurst, J., Jones, T.R., Vernon, S.K., Morin, J., LaRoque, J., Field, B., O'Hara, B., Bloom, J.D., Johann, S.R., 2000. Novel class of thiourea compounds that inhibit herpes simplex virus type 1 DNA cleavage and encapsidation: resistance maps to the UL6 gene. J. Virol. 74, 9054–9061.

Ward, P.L., Ogle, W.O., Roizman, B., 1996. Assemblons: nuclear structures defined by aggregation of immature capsids and some tegument proteins of herpes simplex virus 1. J. Virol. 70, 4623–4631.

Weller, S.K., Carmichael, E.P., Aschman, D.P., Goldstein, D.J., Schaffer, P.A., 1987. Genetic and phenotypic characterization of mutants in four essential genes that map to the left half of HSV-1 UL DNA. Virology 161, 198–210.

Zhang, X., Efstathiou, S., Simmons, A., 1994. Identification of novel herpes simplex virus replicative intermediates by field inversion gel electrophoresis: implication for viral DNA amplification strategies. Virology 202, 530–539.